J Solid State Electrochem (2003) 7: 442–449
DOI 10.1007/s10008-002-0345-9

ORIGINAL PAPER

**Maritza A. Páez · Sonia R. Biaggio
Romeu C. Rocha-Filho · Yorma Sepúlveda
José H. Zagal · Alberto Monsalve · Xiaorong Zhou
Peter Skeldon · George E. Thompson**

On understanding the effect of benzotriazole during barrier-film growth on Al-Cu alloys

Received: 18 June 2002 / Accepted: 10 November 2002 / Published online: 8 May 2003
© Springer-Verlag 2003

Abstract The effect of benzotriazole on the growth of anodic films on aluminium and an Al-3.5 wt% Cu alloy has been examined by transmission electron microscopy (TEM) and electrochemical impedance spectroscopy (EIS). Films grown to relatively high voltages reveal flaws and oxygen-filled voids as a result of the surface morphology and copper enrichment and oxidation at the alloy/film interface. Benzotriazole, apart from increasing the efficiency of anodic film growth on the artificially aged alloy, also reduces the population density of the local features. The impedance response of films formed at relatively low voltages has been used to probe the early influence of benzotriazole on the macroscopic surface as well as flaws of the oxide-covered substrate.

Keywords Anodic films · Anodic oxidation · Al-Cu alloy

Introduction

The role of copper during anodic oxidation of Al-Cu alloys has been the subject of several studies [1, 2, 3, 4, 5, 6, 7, 8, 9]. It is known that copper in solid solution in the alloy enriches to a critical level in a thin layer immediately below the anodic film before oxidation as Cu-O units [5, 7]. The resulting Cu^{2+} ions, having greater mobility relative to Al^{3+} ions under the high field, are ejected at the film/electrolyte interface. Additionally, oxidation of copper clusters at the alloy/film interface is associated with oxygen generation in the thickening alumina film. Similar effects are evident at second-phase material during anodizing; however, in this case, prior enrichment of copper is not necessary in the highly alloyed equilibrium phases. As a result of oxygen generation, gas-filled voids develop with significant pressures exerted on the surrounding alumina film material. Above a critical pressure, the film ruptures and local anodizing heals the defect [10]. Consequently, film growth on the copper-containing alloy proceeds at a significantly reduced efficiency than on aluminium of high purity.

In order to improve the efficiency of anodizing of Al-Cu alloys, additions of benzotriazole (BTA) and thiourea to the anodizing electrolyte have shown some success, with oxygen evolution inhibited during potentiodynamic polarization [11, 12]. In this work, the influence of BTA on anodic film growth on solution heat-treated and artificially aged Al-3.5 wt% Cu alloys has been examined. Film morphology has been revealed by transmission electron microscopy (TEM) of stripped films. Additionally, the influence of BTA on the impedance of the oxide-covered substrate has been examined to gain insight into its general and local behaviour.

M. A. Páez (✉) · Y. Sepúlveda · J. H. Zagal · A. Monsalve
Departamento de Química de los Materiales,
Facultad de Química y Biología,
Universidad de Santiago de Chile,
Casilla 40, Correo 33, Santiago, Chile
E-mail: mpaez@lauca.usach.cl

S. R. Biaggio · R. C. Rocha-Filho
Departamento de Química,
Universidade Federal de São Carlos,
C.P. 676, 13560-970 São Carlos, SP, Brazil

X. Zhou · P. Skeldon · G. E. Thompson
Corrosion & Protection Centre,
University of Manchester Institute of Science and Technology,
Manchester, M60 1QD, UK

Experimental

Specimens of cold-rolled Al-3.5 wt% Cu were either solution heat-treated (808 K/2 h, water quench) or solution heat-treated and aged (808 K/2 h, water quench + 623 K/2 h, water quench). Before anodizing, spade electrodes of superpure aluminium (99.99% Al, 0.004% Fe, 0.003% Cu, 0.002 wt% Si) and Al-3.5 wt% Cu were electropolished for 5 min in a 20/80 v/v perchloric acid/ethanol solution, at 275 K. The surface morphology of the electropolished electrodes was examined in a JEOL 5410 scanning electron microscope, equipped with energy-dispersive X-ray (EDX) analysis facilities. Subsequently, oxide films were grown anodically over the

surface of electropolished electrodes at 15 mA cm^{-2} up to 100 V in a 0.1 M ammonium pentaborate solution, either in the absence or in the presence of benzotriazole (0.08 M), at 293 K. The voltage-time responses for the individual specimens were recorded during anodizing. After anodizing, the oxide films were stripped from the substrate and examined in a JEOL SX-100 transmission electron microscope in order to study the oxide morphologies.

Electrochemical impedance spectroscopy (EIS) measurements were made using a potentiostat/frequency response analyser and software from Eco Chemie. A platinum cylindrical grid counter electrode and a saturated calomel reference electrode (SCE) were used. Previous to the measurements, the oxide films were potentiodynamically formed in a 0.1 M ammonium pentaborate solution, either in the absence or in the presence of BTA (0.08 M) by scanning the potential from −1 V up to 5 V (vs. SCE), at 50 mV s^{-1}, and returning to the initial potential by a cathodic scan. The impedance data for the different Al-Cu alloy/oxide film/electrolyte systems were obtained in the same solution where the film was formed, at a DC potential as close as possible to the open circuit potential of each system (this potential remained in the range −1.0 V to −0.7 V vs. SCE). An AC perturbation of 30 mV rms, in the frequency range 10 mHz to 10 kHz, was used; owing to noise, in some measurements the lower frequency used was 30 mHz instead of 10 mHz.

Results

Surface morphology

Figure 1 shows the surface morphology of electropolished superpure aluminium and the two differently heat-treated Al-Cu alloys. As expected, the electropolished superpure aluminium is featureless, while the electropolished Al-Cu alloys reveal cavities and light regions of different sizes and distributions. The latter regions are evident for the solution-aged heat-treated Al-Cu alloy (see Fig. 1C). In general, EDX analysis (X-ray map) of the solution heat-treated alloy surface (see Fig. 1B) revealed a uniform copper content of about 3.5 wt%, indicating that cavities in this surface possibly represent original microscopic intermetallic particles, which dissolved completely during electropolishing [11, 12]. In contrast, EDX analysis of the solution-aged heat-treated alloy surfaces revealed local high copper contents of about 50 wt% Cu, particularly for probe positions above the larger light regions, which suggests the presence of $CuAl_2$ intermetallic particles.

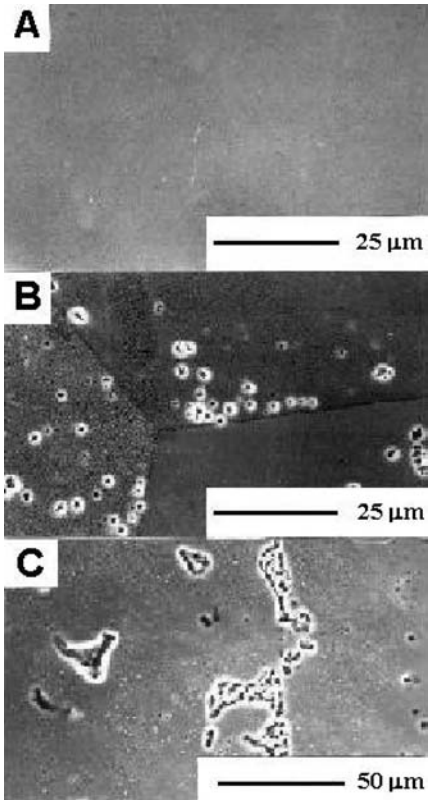

Fig. 1A–C SEM micrographs showing the surface morphology of electropolished aluminium and Al-Cu alloys. **A** 99.99 wt% Al; **B** solution heat-treated Al-3.5 wt% Cu alloy; **C** solution heat-treated and aged Al-3.5 wt% Cu alloy

Differences on the surface appearance of the differently heat-treated Al-Cu alloys are mainly attributed to the distinct sizes and population densities of intermetallic particles in the original surface and, consequently, to the partial or complete dissolution of such regions during electropolishing [11, 12, 13].

Voltage-time behaviour

Figure 2 shows the voltage-time responses during anodizing aluminium of high purity and the differently heat-treated Al-Cu alloys at 15 mA cm^{-2} in 0.1 M ammonium pentaborate solution, in the absence and presence of BTA (0.08 M). This concentration was selected according to previous studies of the authors relating to the effect of BTA on the anodic behaviour of Al-3.5 wt% Cu [13]. Considering the relevant aspects to be discussed here (Fig. 2A and Fig. 2B), additions of BTA do not change the voltage-time responses for superpure aluminium and for the solution heat-treated Al-Cu alloy. In contrast, the voltage-time response of the aged Al-Cu alloy (Fig. 2C) presents two regions of different slopes: an initial region up to 20 V of slope ~1.4 V s^{-1}, followed thereafter by a region of slope ~5.5 V s^{-1}. The initial voltage region of slope 1.4 V s^{-1} is attributed to secondary electrochemical reactions, such as local copper oxidation and oxygen evolution, proceeding above copper-rich regions on the alloy substrate. As revealed in Fig. 1C, such regions are possibly second-phase regions, which result from partial dissolution during the electropolishing [2, 11, 14]. Conversely, in the presence of BTA, the initial region of slope ~1.4 V s^{-1} is not present and the voltage increases from the beginning at a constant rate of ~5.6 V s^{-1}. Assuming an efficiency of 100% for a voltage rise of 7.5 V s^{-1} [15], the low initial slope during anodizing in the absence of the additive implies an initial anodic efficiency of about 19%, while this efficiency is ca. 75% for film formation in the presence of BTA. Thus, the main effect of BTA on anodizing the solution heat-treated/aged Al-Cu alloy is to increase the efficiency for film growth in the initial stages of film formation by a factor of about four.

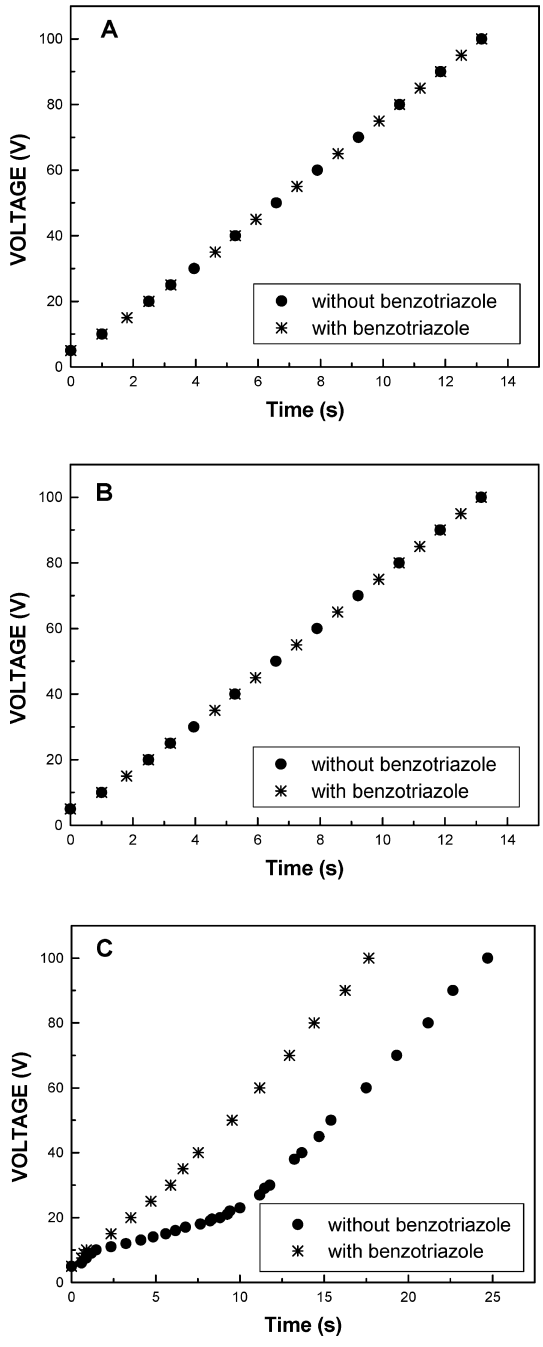

Fig. 2A–C Voltage-time behaviour during anodizing aluminium and the Al-Cu alloys at 150 A m^{-2} in 0.1 M ammonium pentaborate, in the absence and presence of 10 g L^{-1} of benzotriazole. **A** 99.99 wt% Al; **B** solution heat-treated Al-3.5 wt% Cu; **C** solution heat-treated and aged Al-3.5 wt% Cu

Morphology of oxide films grown in ammonium pentaborate solution

Figure 3 (A, C and E) shows transmission electron micrographs of stripped barrier anodic films formed during anodizing the respective electropolished substrates at 15 mA cm^{-2} up to 100 V in a 0.1 M ammonium pentaborate solution. As expected, the anodic film formed on superpure aluminium appears relatively

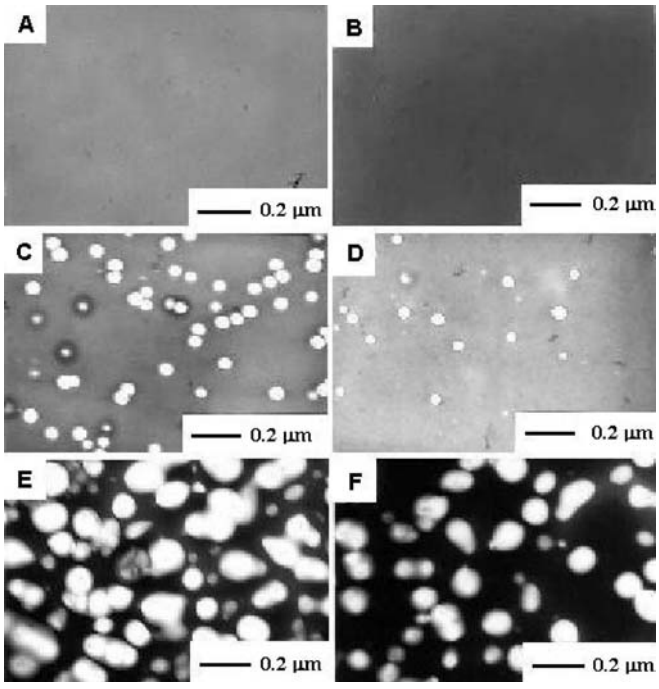

Fig. 3A–F TEM micrographs revealing stripped films formed on the different metal substrates at 150 A m^{-2} up to 100 V in 0.1 M ammonium pentaborate, in the absence and presence of 10 g L^{-1} of benzotriazole. 99.99 wt% Al in the absence (**A**) and in the presence (**B**) of the additive; solution heat-treated Al-3.5 wt% Cu in the absence (**C**) and in the presence (**D**) of the additive; solution heat-treated Al-3.5 wt% Cu in the absence (**E**) and in the presence (**F**) of the additive

featureless, in good agreement with the morphology of the metal substrate shown in Fig. 1A. In contrast, the stripped films formed on the Al-Cu alloys (Figs. 3C and E) reveal high volume fractions of differently contrasted, approximately circular, regions, which are associated with the presence of flaws in the anodic film and/or oxygen-filled voids in the film [3, 7]. For films formed on the solution heat-treated Al-Cu alloys (Fig. 3C), such regions reveal diameters between 0.03 μm and 0.1 μm and a population density of 4.5×10^{13} m^{-2}. From the area of the light regions in Fig. 3C, the fraction of the film associated with flaws is 0.14. For films formed on the solution/aged Al-Cu alloy (Fig. 3E), isolated flaws of diameters up to 0.3 μm are evident, with chains of such features in other regions. Although for this film it is difficult to calculate a population density of flaws, because of the particular shape and area of the flaws, the fraction of film corresponding to flaws is 0.5. From this information, a correlation between oxide morphology and surface morphology is revealed. Thus, while anodic films on superpure aluminium are featureless as a result of the original smooth surface (Fig. 1A), films grown on the Al-Cu alloys are flawed in appearance. In addition, comparing the films formed on the differently heat-treated Al-Cu alloys, the flaw size is clearly dependent on the particular heat treatment undergone by the alloy and is of greater values for those formed on anodizing the solution/aged heat-treated Al-Cu alloy.

Morphology of oxide films grown in the presence of benzotriazole

Micrographs of the films formed on the electropolished metal substrates in 0.1 M ammonium pentaborate with addition of BTA (0.08 M) are shown in Fig. 3 (B, D and F). It can be seen that the general appearance of the anodic films formed on the different metal substrates is not influenced by additions of BTA to the anodizing electrolyte. Thus, light regions related to flaws are also revealed in films formed in the presence of the additive. However, when comparing the micrographs in Fig. 3D and Fig. 3F with the corresponding micrographs in Fig. 3C and Fig. 3E, it is clear that additions of BTA to the anodizing electrolyte reduce the fraction of the films corresponding to flaws. Thus, for the film formed on the solution heat-treated Al-Cu alloy, the fraction of the films is reduced from 0.14 to 0.026, while for the film formed on the aged Al-Cu alloys, it is reduced from 0.5 to 0.25. Further, from the *V-t* responses for the solution/aged Al-Cu alloy (Fig. 2C), the effect of BTA in reducing flaw generation appears to be associated with a greater anodic efficiency, as revealed by the higher initial rate of voltage rise obtained during anodizing the alloy in the presence of BTA. In contrast, from the *V-t* responses for the solution heat-treated Al-Cu alloy (Fig. 2B), the influence of BTA in decreasing flaw sizes during anodizing does not seem to be associated with a change in the initial rate of voltage rise. This, as discussed later, is possibly associated with causes originating the flaws, specifically critical sizes and local compositions of different features in the metal substrate affecting the initial anodic efficiency.

Impedance measurements

To further understand the influence of BTA on the anodizing of the differently heat-treated Al-Cu alloys, EIS measurements of the Al-Cu/anodic film/electrolyte systems were carried out in 0.1 M ammonium pentaborate, either in the absence or in the presence of the additive. To gain additional insight on the influence of copper in the resulting impedance response, similar measurements were also carried out on the superpure aluminium/anodic film/electrolyte system. The anodic films were potentiodynamically formed and the impedance data were obtained in the same solution where the film was formed, at a DC potential as close as possible to the open circuit potential of each system.

Impedance data in the absence of benzotriazole

Typical Bode plots of the impedance data obtained for the superpure aluminium/anodic film/electrolyte system and the Al-Cu/anodic film/electrolyte systems in a 0.1 M ammonium pentaborate solution are shown in Fig. 4. Differences in the impedance response of the three electrodes are evident over most of the frequency range studied (Fig. 4A). For almost all frequencies, the values of the impedance modulus of the Al-Cu/anodic film systems are higher than those for the superpure aluminium/anodic film system. Furthermore, the highest values of the impedance modulus are those of the solution heat-treated Al-Cu alloy. At the lowest frequencies, the value of the impedance modulus of the solution-aged heat-treated Al-Cu alloy tends to become the lowest of the three systems studied.

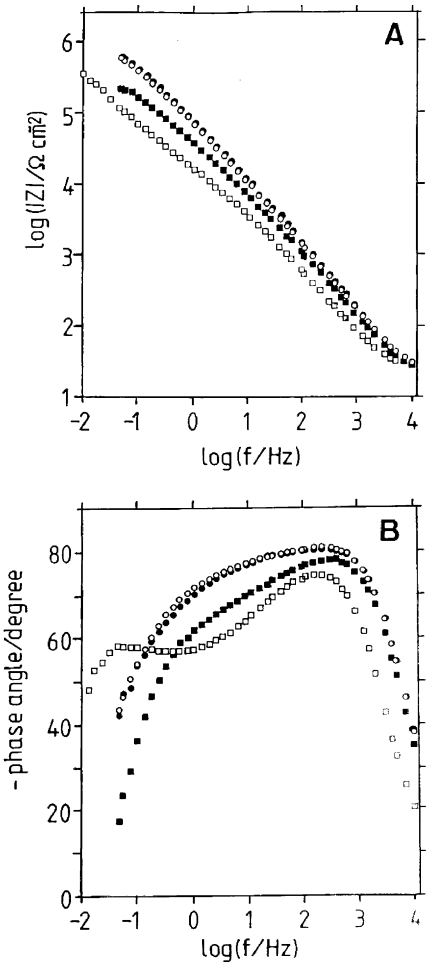

Fig. 4 Bode plots of the impedance (**A**) and phase angle data (**B**) obtained for the metal substrate/anodic film/electrolyte system in 0.1 M ammonium pentaborate solution at −1.0 V (SCE). *Open squares*: 99.99 wt% Al; *filled squares*: solution-aged heat-treated Al-Cu alloy; *open circles*: solution heat-treated Al-Cu alloy; *filled circles*: fitted impedance values for the solution heat-treated Al-Cu alloy

The phase angle Bode plots (Fig. 4B) clearly show that the impedance response is frequency distributed, even for the Al system, most probably due to a dispersion in the time constants of the measured responses. In the case of the Al electrode, two separate distributed time constants are quite evident, but those are not clearly revealed for the Al-Cu systems. However, two separate

distributed time constants for the Al and Al-Cu systems were evident when the data for the different systems were fitted to the transfer function corresponding to the equivalent circuit shown in Fig. 5, using a non-linear least-squares procedure (Boukampt's equivalent circuit software, version 4.55). In this equivalent circuit, the components of the circuit represent: the electrolyte resistance (R_S), the resistance (R_1) and the distributed capacitive behaviour (Q_1) (constant phase element) associated with the barrier film; and the resistance (R_2) and the distributed capacitive behaviour (Q_2) (constant phase element) associated with film areas acting as easy paths for the passage of current. The values of the different parameters obtained through the non-linear least-squares fitting of the transfer function to the different impedance data are given in Table 1. For illustrative purposes, the fitted data for the heat-treated Al-Cu alloy is presented in Fig. 4. The close correspondence between experimental and fitted data indicates that the chosen transfer function describes the behaviour of the system rather well. A similar correspondence between experimental and fitted data was found for the heat-treated Al-Cu alloy and for the superpure aluminium. The impedance measurements of the different metal oxide/electrolyte systems indicate that additions of copper to aluminium increase the impedance of the anodic film. This may be the result of the copper-enriched layer at the alloy/film interface, formed potentiodinamically during the anodic scan. The copper enrichment at the alloy/film interface is expected to influence both the ionic and, consequently, the electronic resistance of the alloy/oxide/electrolyte system.

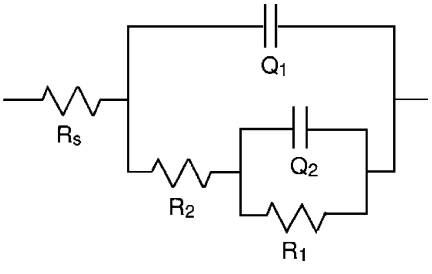

Fig. 5 Equivalent circuit representing the impedance behaviour of the aluminium/oxide/electrolyte system

Impedance data in the presence of benzotriazole

Typical Bode plots of the impedance data obtained for the superpure aluminium/anodic film/electrolyte system and the Al-Cu/anodic film/electrolyte systems in a 0.1 M ammonium pentaborate solution, in the absence and presence of 0.08 M of BTA, are shown in Fig. 6. As observed, additions of BTA to the electrolyte do not significantly change the impedance behaviour of the three metal/anodic film/electrolyte systems in the high-frequency region. However, in the low-frequency region, the presence of the additive increases the impedance modulus of the three systems studied. The increase is greater for the solution/aged heat-treated Al-Cu alloy. The fitting of the data shown in Fig. 6 to the transfer function corresponding to the equivalent circuit shown in Fig. 5, using a non-linear least-squares procedure, is also rather good, as illustratively shown in the figure for the heat-treated Al-Cu alloy. Further, for the case of the two differently heat-treated Al-Cu alloys, the values for R_1 and R_2 (see Table 1), representing respectively the resistances of the oxide film and of the metal regions associated with the easy path for the passage of current, are increased in the presence of the additive.

The impedance response in the low-frequency region of aluminium and its oxide, formed either by chemical or galvanostatic or potentiodynamic oxidation, has been interpreted before in terms of conductive sites associated with impurities and alloying element segregates [16, 17]. The effect of BTA in increasing the impedance modulus of the Al-Cu alloy electrodes in the low-frequency region may be the result of local compositional changes and/or a decrease in the size and population density of conductive sites in the metal substrate.

Discussion

Role of benzotriazole in reducing the effect of copper-rich regions on anodizing Al-Cu alloys

Clearly the main difference between the anodizing response of the differently heat-treated Al-Cu alloys in ammonium pentaborate solutions is attributed to the absence or presence of intermetallic particles. The presence of intermetallic particles, mainly $CuAl_2$, promotes

Table 1 Dependence of fitting parameters on the type of metallic substrate anodized and electrolyte used, obtained using the transfer function for the circuit depicted in Fig. 5 (for meaning of the parameter symbols, see text)

Metal substrate[a] and electrolyte[b]	R_s (Ω cm^2)	R_1 (MΩ cm^2)	Q_1 (μF cm^2 s^{n-1})	n_1	R_2 (kΩ)	Q_2 (μF cm^2 s^{n-1})	n_2
Al in APB solution	23	1.0	5.9	0.88	13	13	0.73
Al in APB + BTA solution	25	1.0	7.0	0.88	14	16	0.67
SHT Al-Cu alloy in APB solution	22	1.3	1.5	0.95	7.8	1.7	0.64
SHT Al-Cu alloy in APB + BTA solution	34	2.9	1.8	0.95	49	1.7	0.68
SAHT Al-Cu alloy in APB solution	20	0.25	2.5	0.92	14	3.4	0.73
SAHT Al-Cu alloy in APB + BTA solution	22	0.95	2.2	0.93	33	2.6	0.67

[a]Al, 99.99 wt% Al; SHT Al-Cu, solution heat-treated Al-Cu alloy; SAHT, solution/aged heat-treated Al-Cu alloy
[b]APB, 0.1 M ammonium pentaborate solution; BTA, 10 g L^{-1} benzotriazole

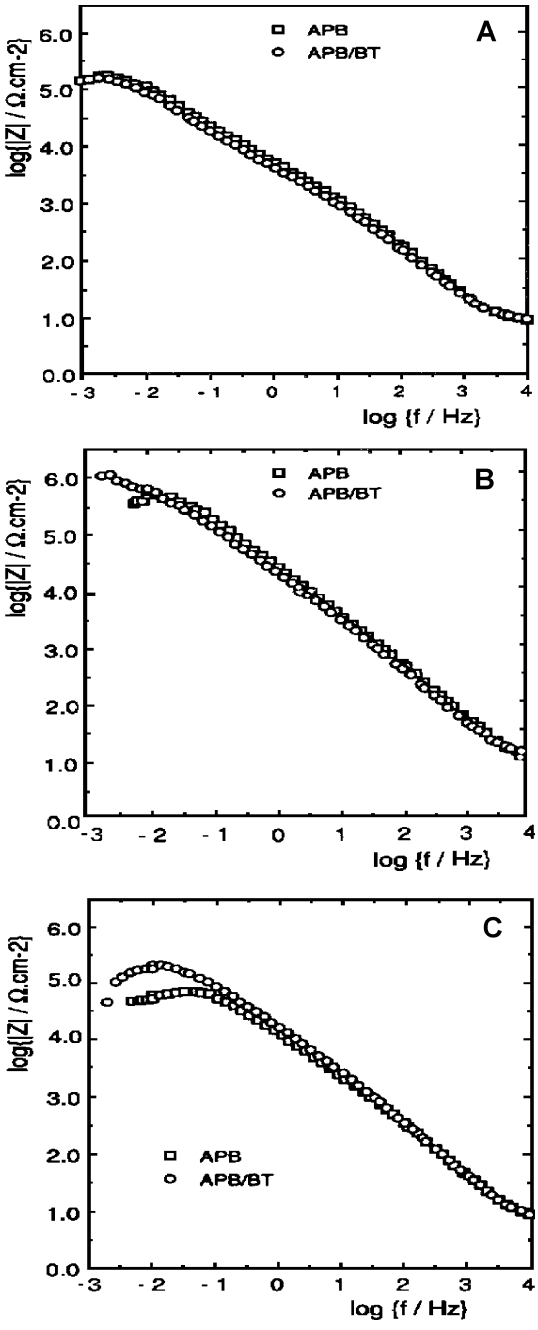

Fig. 6A–C Bode plots of the impedance obtained for the metal substrate/anodic film/electrolyte system in 0.1 M ammonium pentaborate solution at −1.0 V (SCE) in the absence and presence of 10 g/L of benzotriazole. **A** 99.99 wt% Al; **B** solution heat-treated Al-Cu alloy; **C** solution-aged heat-treated Al-Cu alloy

the execution of secondary electrochemical reactions, such as oxygen evolution, which was visually observed. Generally, the likely sites for oxygen generation on aluminium are impurities, alloying elements segregates and second phases [18]. Above these regions the natural oxidation of aluminium is limited and the absence or the presence of a locally contaminated air-formed oxide can be envisaged. The size and population density of these regions are dependent on the composition of the metal substrate and on the surface treatment and heat treatment given to the aluminium prior to anodizing [16]. In the case of aluminium alloys of relatively high copper content, such regions are related to intermetallic particles, mainly θ and θ' [1, 11, 19]. The absence or the presence of a very thin contaminated air-formed oxide above these regions allows the passage of an electronic current, which is anticipated to be sufficiently high to assist locally secondary charge-transfer reactions. The extension of the reactions consuming charge will depend on the size and population density of the intermetallic particles. In any case, large regions assisting alternative reactions will result in a retardation of the voltage rise in the initial stages of anodizing, because of a reduction in the effective current density for film formation. Then, the period at 7 V at the commencement of anodizing the solution-aged aluminium alloy is the result of one or a combination of an increased electronic current and a reduced field for ionic current. From the *V-t* response, the voltage starts rising with further anodizing, indicating that bridging over into the film occurs. The manner that film growth is repaired locally is not discussed here, but it is highly possible that oxygen evolved above such regions reduces the electronic conduction, owing to its insulating characteristic; the resulting gas may be trapped by the film bridging over it [19].

The influence of benzotriazole in the initial stages of anodizing the aged Al-Cu alloy is to shorten markedly the secondary electrochemical reactions and consequently to increase the efficiency for film formation. Assuming an interrelationship with the area of the conductive sites associated with intermetallic particles, clearly the additive reduces the size of such regions. Further, considering its effect at the commencement of anodizing, such a reduction in area occurs immediately after immersion of the alloy in the electrolyte.

In the case of the solution heat-treated Al-Cu alloy, additions of benzotriazole to the anodizing electrolyte have a non-apparent effect on the voltage-time behaviour, implying the absence of conductive sites associated with intermetallic particles. Although the presence of microscopic conductive sites associated with GP zones are expected, regarding the natural ageing process of the alloy at room temperature and the high copper content in the alloy, their area and consequently the passage of electronic current through such surface sites is considered to be negligible. Therefore, there is an interplay between the likely sites of copper-rich regions with regards to their sizes and local compositions and the extent of secondary electrochemical reactions, reducing markedly the effective current density and retarding the voltage rise in the initial stage of anodizing.

The role of the surface morphology on the voltage-time response in the initial stages of Al-Cu alloys is further revealed by the impedance measurements of the differently heat-treated alloy systems. The expected extremely thin oxide formed potentiodinamically reproduces the surface of the alloy prior to anodizing. Over 10 Hz, there are not significant differences between the

impedance response of the differently heat-treated Al-Cu alloys (Fig. 4); however, below that frequency value, a lower impedance modulus for the aged Al-Cu alloy is evident. Generally, for aluminium substrates the impedance response in the low-frequency region has been associated with flaws in the metal substrate, which represents regions of low resistance for the passage of current [16, 17, 20, 21]. The lower impedance of the aged Al-Cu alloy may then be attributed to the presence of intermetallic particles in the metal substrate.

Additions of benzotriazole increase exactly the impedance response in the low-frequency region, confirming that its effect is mainly to increase the resistance of copper-rich regions associated with intermetallic particles. Although the data in Table 1 do not provide absolute resistance values, it indicates their relative variance resulting from additions of benzotriazole. The increase of the electrical resistance of conductive sites is attributed to the local formation of a protective film on the electrode surface. Owing to the local high copper content and the ability of benzotriazole to react with Cu^+ ions, the formation of a protective film constituted by a cuprous benzotriazole complex, Cu-BTA, can be anticipated. On copper electrodes, such a protective film has been characterized by XPS, Raman [22, 23, 24] and TEM of ultramicrotomed sections of copper (Shimizu K, unpublished results). The Cu-BTA complex on copper electrodes forms a chemisorbed layer at low coverage and a multilayer polymerized structure at larger film thicknesses [25, 26]. The details of the mechanism by which the film forms and protects the metal are the subject of much investigation and debate. In sulfate solutions, a 0.01 M BTAH concentration inhibits corrosion of copper in the pH range 2–12, and is particularly effective in the pH range 4–10 [27]. The pH of 0.1 M ammonium pentaborate solution is 7.6, which is in the range where benzotriazole has its major reactivity with Cu^+ ions. From previous work of the authors, copper oxides are immediately formed during potentiodynamic oxidation of Al-Cu alloys [12, 13]. The conditions for the additive to react locally above copper-rich regions are thus given.

Role of benzotriazole in reducing flaw development during anodizing

Besides the effect of benzotriazole in reducing faradic processes in the initial stages of anodizing, the additive also decreases the events associated with flaw development, as revealed in the TEM micrographs of Fig. 3. Considering this, the causes of the flaws during anodic oxidation of aluminium and its alloys, with regards to their effects in the film morphology, are reviewed. The two major contributions to flaw generation in anodic film on aluminium alloys have been associated with the surface morphology of the alloy [15, 18] and with the alloying elements behaviour during anodic oxidation of the alloys [7, 19]; generally for anodizing to high voltages, a combined influence of both contributions is expected.

Considering the influence of the surface morphology, the likely sites for flaw generation on aluminium are impurities, alloying elements segregates and second phases. Thus, the size and population density of the flaws are dependent on the composition of the metal substrate and on the surface treatment and heat treatment given to the aluminium prior to anodizing. The population density of flaws in films formed on electropolished aluminium of high purity in ammonium pentaborate solution is about 10^{-8} m^{-2} [18]. The uniform film revealed in Fig. 3A is thus the result of a relatively low population density of such features and the small film surface examined in the transmission electron microscope. Regarding the previous information, the presence of flaws in anodic films formed on the Al-Cu alloys and thereby the contribution of the heat-treatment procedure to the flaw size and population density is not surprising. According to Young [19], flaws in anodic films are associated with trapping of oxygen gas by the film bridging over it; oxygen is generated above impurities and alloying element segregates.

Concerning the influence of alloying elements promoting flaws in anodic films on aluminium, the copper behaviour during anodizing the Al-Cu alloys is also expected to contribute to the development of such features. These have been also associated mainly with oxygen-filled voids in the anodic film [7], but the manner and the mechanism of their formation is different to that proposed by Young [19]. The interplay between the development of oxygen-filled voids in the anodic film and copper enrichment at the metal/oxide interface, resulting from surface treatments and maintained further during anodizing, has been reported in several papers of the authors [2, 7, 10]. The mechanism of oxygen-filled void formation during galvanostatic oxidation of Al-Cu is sustained on the inward movement of O^{2-} ions to reach semiconductive sites formed by local oxidation of copper at the copper-enriched layer. Because of the necessary ionic migration and copper oxidation at the alloy/film interface, this contribution to flaw development is of major importance for anodizing to voltages above 20 V.

Based on the analysis of causes originating flaws in anodic films, the influence of benzotriazole appears more related to the effect of the surface morphology promoting flaws than to the effect of copper behaviour during anodizing assisting the formation of oxygen-filled voids. This considers the unavoidable copper enrichment at the alloy/film interface and inward migration of O^{2-} ions during galvanostatic oxidation of aluminium to high voltages and, further, the limited incorporation and inward migration of benzotriazole anions in the film. Although anion derivatives of benzotriazole, generated at the oxide/electrolyte interface through loss of H^+ ions from the molecule, may be incorporated into the outer layer of the anodic film, their incorporation into the film is limited. This considers the presence of borate species

in the oxide/electrolyte interface and the well-known incorporation of these species into the anodic film [18]. Nevertheless, benzotriazole may assist healing processes during local cracking of the film, which would leave the copper enrichment exposed to the electrolyte, but this is considered to be of major importance only for anodizing to voltages higher than 100 V [7].

Conclusions

Firstly, additions of BTA to the anodizing electrolyte increase the efficiency for barrier film formation on solution/aged Al-Cu alloys in the initial stages of anodizing. Such an increase is mainly due to an increase in the resistance of conductive sites associated with intermetallic particles in the metal substrate.

Secondly, additions of BTA to the anodizing electrolyte decreases flaw generation events, reducing the size and population density of flaws in anodic films on the Al-Cu alloy. The additive, by its local adsorption above impurities, copper segregates and second phases, limits the local passage of electronic current assisting oxygen gas evolution and reduces the probability of oxygen gas trapping in the film.

Thirdly, the increase in the resistance of conductive surface sites in the metal substrate is apparently the result of the formation of a polymeric film, namely Cu-BTA, above copper-rich regions.

Acknowledgements Financial support from DICYT (USACH) and FONDECYT (grant 80100006), Chile, is gratefully acknowledged. A grant from the CNPq (Brazil)/CONICYT (Chile) Co-operation Programme is also gratefully acknowledged. Our thanks to Eng. O. Perez for his useful comments in the preparation of this paper.

References

1. Wood GE, Brock AJ (1966) Trans Inst Metal Finish 44:189
2. Páez MA, Foong TM, Ni CT, Thompson GE, Shimizu K, Habazaki H, Skeldon P, Wood GC (1996) Corros Sci 38:59
3. Habazaki H, Shimizu K, Páez MA, Skeldon P, Thompson GE, Wood GC, Zhou X (1995) Surf Interface Anal 23:892
4. Habazaki H, Páez MA, Shimizu K, Skeldon P, Thompson GE, Wood GC, Zhou X (1996) Corros Sci 38:1033
5. Zhou X, Thompson GE, Habazaki H, Shimizu K, Skeldon P, Wood GC (1997) Thin Solid Films 293:327
6. Habazaki H, Zhou X, Shimizu K, Skeldon P, Thompson GE, Wood GC (1997) Electrochim Acta 42:2627
7. Skeldon P, Thompson GE, Wood GC, Zhou X, Habazaki H, Shimizu K (1997) Philos Mag A 76:729
8. Solomon JS, Hanlin DE (1980) Appl Surf Sci 4:307
9. Strehblow HH, Melliar-Smith CM, Augustyniak WM (1978) J Electrochem Soc 125:15
10. Thompson GE, Habazaki H, Páez MA, Shimizu K, Skeldon P, Wood GC (2000) J Electrochem Soc 147:1747
11. Páez MA (1992) PhD Thesis, University of Manchester, Institute of Science and Technology, Manchester, UK
12. Páez MA, Thompson GE, Bustos O, Zagal JH, Skeldon P (1997) J ATB Metall 37:179
13. Páez MA, Zagal JH, Bustos O, Aguirre MJ, Skeldon P, Thompson GE (1997) Electrochim Acta 42:3453
14. Páez MA, Bustos O, Thompson GE, Skeldon P, Shimizu K, Wood GC (2000) J Electrochem Soc 147:1015
15. Harkness AC, Young L (1966) Can J Chem 44:2409
16. Richardson JA, Wood GC, Sutton WH (1973) Thin Solid Films 16:99
17. Xu N, Thompson GE, Dawson JL, Wood GC (1993) Corros Sci 34:479
18. Thompson GE, Wood GC (1983) Anodic films on aluminium. In: Scully JC (ed) Treatise on materials science and technology, vol 23. Academic Press, London, pp 205–329
19. Young L (1961) Acta Metall 5:711
20. Bessone J, Mayer C, Jüttner K, Lorenz WJ (1983) Electrochim Acta 28:171
21. Xue G, Ding J, Cheng P (1985) Appl Surf Sci 89:77
22. Hobbins ND, Roberts RF (1979) Surf Technol 9:235
23. Thompkins GH, Sharma SP (1982) Surf Interface Anal 4:261
24. Lewis ML, Carron KT (1993) Langmuir 9:186
25. Metikos-Hukovic M, Rabic R, Murinovic A (1998) J Electrochem Soc 145:4045
26. Babic R, Metikos-Hukovic M, Loncar M (1999) Electrochim Acta 14:2413
27. Brusic V, Frish MA, Eldrigge BM, Novak FP, Krufman FP, Bush BM, Frankel GS (1991) J Electrochem Soc 138:2233